Journal of Neurology (2022) 269:4404–4413
https://doi.org/10.1007/s00415-022-11081-3

ORIGINAL COMMUNICATION

Clusters of anatomical disease-burden patterns in ALS: a data-driven approach confirms radiological subtypes

Peter Bede[1] · Aizuri Murad[1] · Jasmin Lope[1] · Orla Hardiman[1] · Kai Ming Chang[1,2]

Received: 10 February 2022 / Revised: 10 March 2022 / Accepted: 11 March 2022 / Published online: 25 March 2022

Abstract

Amyotrophic lateral sclerosis (ALS) is associated with considerable clinical heterogeneity spanning from diverse disability profiles, differences in UMN/LMN involvement, divergent progression rates, to variability in frontotemporal dysfunction. A multitude of classification frameworks and staging systems have been proposed based on clinical and neuropsychological characteristics, but disease subtypes are seldom defined based on anatomical patterns of disease burden without a prior clinical stratification. A prospective research study was conducted with a uniform imaging protocol to ascertain disease subtypes based on preferential cerebral involvement. Fifteen brain regions were systematically evaluated in each participant based on a comprehensive panel of cortical, subcortical and white matter integrity metrics. Using min–max scaled composite regional integrity scores, a two-step cluster analysis was conducted. Two radiological clusters were identified; 35.5% of patients belonging to 'Cluster 1' and 64.5% of patients segregating to 'Cluster 2'. Subjects in Cluster 1 exhibited marked frontotemporal change. Predictor ranking revealed the following hierarchy of anatomical regions in decreasing importance: superior lateral temporal, inferior frontal, superior frontal, parietal, limbic, mesial inferior temporal, peri-Sylvian, subcortical, long association fibres, commissural, occipital, 'sensory', 'motor', cerebellum, and brainstem. While the majority of imaging studies first stratify patients based on clinical criteria or genetic profiles to describe phenotype- and genotype-associated imaging signatures, a data-driven approach may identify distinct disease subtypes without a priori patient categorisation. Our study illustrates that large radiology datasets may be potentially utilised to uncover disease subtypes associated with unique genetic, clinical or prognostic profiles.

Keywords Amyotrophic lateral sclerosis · Neuroimaging · Biomarkers · Motor neuron disease · Diffusion imaging · Clinical trials

Introduction

Clinical heterogeneity in ALS is widely recognised. While the diagnosis of ALS requires a core set of clinical features, considerable differences exist in progression rates, disability profiles, survival, cognitive manifestations, and behavioural features [1–4]. Key dimensions of clinical heterogeneity include LMN versus UMN predominance, body region of symptom onset and cognitive profiles, but less characteristic symptoms, such as extrapyramidal, cerebellar, and sensory deficits may also add to the diversity of clinical manifestations [5–8]. The practical upshot of clinical heterogeneity includes the considerable differences in care needs, support services, caregiver burden and resources needed for the multidisciplinary management of the condition. It is widely recognised that individualised supportive strategies are required for the optimal management of ALS, and it is also increasingly accepted the individualised pharmacotherapy may be needed instead of the traditional "one-drug-for-all" approach. The ramifications of disease heterogeneity span beyond patient care and are a considerable challenge in clinical trials which are often hampered by small cohort sizes, stringent entry criteria and high drop-out rates [9]. In line with the concepts of precision medicine, and in recognition of the diversity of clinical trajectories in ALS, a multitude of classification schemes and staging systems were

✉ Peter Bede
bedep@tcd.ie

[1] Computational Neuroimaging Group, Trinity Biomedical Sciences Institute, Trinity College Dublin, Pearse Street, Room 5.43, Dublin 2, Ireland

[2] Department of Electronics and Computer Science, University of Southampton, Southampton, UK

introduced to categorise patient with similar disability, prognostic or cognitive profiles [10–14]. These staging systems are relatively easy to apply in the clinical setting, useful in pharmacological trials, and proved successful in reducing clinical diversity by allocating patients into specific disease categories. Clinical staging, however, require the careful consideration of observed parameters and invariably rely on the interpretation of medical cues, reported symptoms and other potentially subjective factors. An alternative to clinical staging is the exploration of quantitative biomarker data [15–17] to evaluate if distinct subgroups exist, using a data-driven approach relying solely on quantitative, "measured" variables. While the majority of imaging studies use clinical categorisation first to then describe phenotype-, genotype- or stage-associated radiological profiles [18, 19], an alternative is the cluster analysis of pooled imaging data and the subsequent analysis of cluster-associated clinical characteristics. Accordingly, the main objective of this study is the evaluation of a large unsegregated MR dataset with regards to radiological clusters of anatomical involvement without a priori patient categorisation. Our hypothesis is that disease subtypes may be readily identified using a data-driven approach without relying on accompanying clinical variables. A secondary objective of the study is the interrogation of cluster-associated demographic, clinical and genetic information once cluster membership has been established for each participant.

Methods

Participants

A total of 214 patients with amyotrophic lateral sclerosis (ALS) were included in a prospective, single-centre study. The study was approved by the institutional ethics board (Beaumont Hospital, Dublin, Ireland), and all participants provided informed consent. Exclusion criteria included prior cerebrovascular events, traumatic brain injury, neurosurgical procedures, as well as comorbid neoplastic, paraneoplastic or neuroinflammatory diagnoses. Participating ALS patients were diagnosed according to the El Escorial criteria. 161 patients were screened for GGGGCC hexanucleotide expansions in *C9orf72*. Methods for genetic screening have been previously reported [20]. GGGGCC repeat expansions in *C9orf72* longer than 30 repeats were considered pathological.

Magnetic resonance imaging

A standardised imaging protocol was implemented on a 3 Tesla Philips Achieva Magnetic resonance (MR) platform. T1-weighted (T1w) images were acquired with a 3D Inversion Recovery prepared Spoiled Gradient Recalled echo (IR-SPGR) sequence with a spatial resolution of 1 mm^3, field-of-view (FOV) of $256 \times 256 \times 160$ mm, flip angle = 8°, SENSE factor = 1.5, TR/TE = 8.5/3.9 ms, TI = 1060 ms. Diffusion tensor images (DTI) were acquired with a spin-echo echo planar imaging (SE-EPI) pulse sequence using a 32-direction Stejskal-Tanner diffusion encoding scheme; 60 slices with no interslice gap, spatial resolution = 2.5 mm^3, FOV = $245 \times 245 \times 150$ mm, TR/TE = 7639/59 ms, SENSE factor = 2.5, *b*-values = 0, 1100 s/mm^2, dynamic stabilisation and spectral presaturation with inversion recovery (SPIR) fat suppression. To assess for comorbid vascular and neuroinflammatory pathologies, an Inversion Recovery Turbo Spin Echo (IR-TSE) sequence was used to acquire FLAIR images, which were systematically reviewed for each participant. FLAIR data were acquired in axial orientation: spatial resolution = $0.65 \times 0.87 \times 4$ mm, 30 slices with 1 mm gap, FOV = $230 \times 183 \times 150$ mm, TR/TE = 11,000/125 ms, TI = 2800 ms, 120° refocusing pulse, with flow compensation and motion smoothing and a saturation slab covering the neck region.

Cortical thickness values

The pre-processing of T1-weighted data included non-parametric non-uniform intensity normalisation, affine registration to the MNI305 atlas, intensity normalisation, skull striping, automatic subcortical segmentation, linear volumetric registration, neck removal, tessellation of the grey matter-white matter boundary, surface smoothing, inflation to minimise metric distortion, and automated topology correction [21]. The anatomical labels of the Desikan–Killiany atlas [22] were used to calculate average cortical thickness in the following cortical regions in the left and right cerebral hemispheres separately: (1) banks superior temporal sulcus, (2) caudal anterior cingulate cortex, (3) caudal middle frontal gyrus, (4) cuneus cortex, (5) entorhinal cortex, (6) frontal pole, (7) fusiform gyrus, (8) inferior parietal cortex, (9) inferior temporal gyrus, (10) insula, (11) isthmus–cingulate cortex, (12) lateral occipital cortex, (13) lateral orbitofrontal cortex, (14) lingual gyrus, (15) medial orbital frontal cortex, (16) middle temporal gyrus, (17) parahippocampal gyrus, (18) paracentral lobule, (19) pars opercularis, (20) pars orbitalis, (21) pars triangularis, (22) pericalcarine cortex, (23) postcentral gyrus (24) posterior-cingulate cortex, (25) precentral gyrus, (26) precuneus cortex, (27) rostral anterior cingulate cortex, (28) rostral middle frontal gyrus, (29) superior frontal gyrus, (30) superior parietal cortex, (31) superior temporal gyrus, (32) supramarginal gyrus, (33) temporal pole, and (34) transverse temporal cortex.

Volume metrics

The brainstem was segmented with a Bayesian parcellation approach into the medulla oblongata, pons, midbrain and superior cerebellar peduncle, based on a probabilistic brainstem atlas derived from 49 scans [23]. A total of 25 volume variables were estimated from each pre-processed T1-weighted dataset: (1) left cerebellar cortex volume, (2) left thalamus volume, (3) left caudate volume, (4) left putamen volume, (5) left pallidum volume, (6) left accumbens volume, (7) left amygdala, (8) left hippocampus, (9) right cerebellar cortex volume, (10) right thalamus volume, (11) right caudate volume, (12) right putamen volume, (13) right pallidum volume, (14) right accumbens volume, (15) right amygdala, (16) right hippocampus, (17) posterior corpus callosum volume, (18) middle corpus callosum volume, (19) central corpus callosum volume, (20) mid-anterior corpus callosum volume, (21) anterior corpus callosum volume, (22) medulla volume, (23) pons volume, (24) superior cerebellar peduncle volume, and (25) midbrain volume, and the total intracranial volume (TIV) was also estimated for each subject. Each volume value was converted as a percentage of the subject's total intracranial volume (TIV) to account for TIV variations.

White matter indices

Following quality control, eddy current corrections and skull removal were applied to DTI data before a tensor model was fitted to generate diffusivity maps of fractional anisotropy (FA). FMRIB's software library's (v6.0) tract-based statistics (TBSS) module was implemented for the non-linear registration of DTI images, skeletonisation and the creation of a mean FA mask. The study-specific white matter skeleton was masked in MNI space by the anatomical labels of the following white matter regions: left and right anterior thalamic radiation, left and right posterior thalamic radiation, left and right cerebellar white matter skeleton, left and right corticospinal tract, forceps major, body of the corpus callosum, forceps minor, left and right inferior cerebellar peduncle, middle cerebellar peduncle, left and right superior cerebellar peduncle, left and right inferior longitudinal fasciculus, left and right uncinate fasciculus, left and right superior frontal lobe, left and right inferior frontal lobe, left and right temporal lobe, left and right occipital lobe, left and right parietal lobe, left and right cingulum, left and right inferior fronto-occipital fasciculus, left and right superior longitudinal fasciculus, left and right medial lemniscus, fornix, and brainstem. To generate spatial masks for the cerebellar peduncles, medial lemniscus and posterior thalamic radiation, the labels of the ICBM-DTI-81 white matter atlas [24, 25] were used. To create masks for the cingulum, forceps major, forceps minor, body of corpus callosum, anterior thalamic radiation, uncinate, inferior longitudinal fasciculi, superior longitudinal fasciculi, inferior fronto-occipital fasciculi, and corticospinal tracts, the labels of the JHU white matter tractography atlas [26, 27] were utilised. FMRIB's fornix template [28] was used to mask the study-specific white matter skeleton in MNI space. Labels of the MNI probabilistic atlas [29, 30] was used to generate a white masks for the cerebellum, frontal, temporal, occipital, and parietal lobes. The frontal lobe was divided into inferior and superior sections at MNI coordinate $z = 8$. Label 8 of the Harvard–Oxford probability atlas [31] was used to create a brainstem mask.

Statistical interpretation

Fifteen key regions of interest (ROIs) were defined covering the entire cerebrum: (1) inferior frontal, (2) superior frontal, (3) peri-Sylvian (lateral sulcus), (4) mesial inferior temporal, (5) superior lateral temporal, (6) parietal, (7) occipital, (8) "motor", (9) commissural, (10) brainstem, (11) cerebellum, (12) subcortical, (13) limbic, (14) long association fibres, and (15) "sensory". A total of 25 volumetric variables, 68 cortical thickness values and 40 white matter indices were systematically retrieved from each subject's imaging data. Integrity metrics of bilateral structures were averaged pairwise, resulting in a total of 74 variables (17 volumes, 34 thickness, 23 FA) in each subject (Table 1). In each anatomical region, cortical thickness values were added and min–max normalised to a 0–1 scale. In subcortical and infratentorial ROIs (corpus callosum, basal ganglia, brainstem, cerebellum etc.), volume values were added and min–max normalised instead. With the exception of the long association ROI, where the two input FA values were 0–1 scaled separately, white matter metrics in each other ROI were added and 0–1 scaled. As a result, in each ROI there were two 0–1 scaled indices which were added for a single composite score representing the integrity of the ROI ranging from 0 to 2, higher scores indicating superior regional integrity, lower scores representing degenerative change.

Based on the 15 regional integrity scores, a 2-step cluster analysis was conducted using Euclidean distance measure. The number of clusters was not fixed a priori, and the Bayesian Information Criterion (BIC) was used to determine the number of clusters. Based on cluster membership of individual patients, cluster sizes were determined and silhouette analyses run using the STATS CLUS SIL extension of SPSS. The hierarchy of input variables was calculated to rank predictor importance, i.e. the measures of which brain regions best segregate the patients. Cluster membership was plotted in a scatter plot along the integrity gradient of the three most relevant ROI to demonstrate case separation. In post hoc

Table 1 Definition of regions of interest and input imaging variables

	ROI	Cortical thickness/volume metrics	White matter metrics
1	Inferior frontal	Lateral orbitofrontal th. Medial orbitofrontal th. Pars orbitalis th. Frontal pole th. Rostral anterior cingulate th.	Inferior frontal FA
2	Superior frontal	Superior frontal th. Rostral middle frontal th. Caudal middle frontal th. Caudal anterior cingulate th.	Superior frontal FA
3	"Peri-Sylvian"	Pars opercularis th. Pars triangularis th. Insula th.	Uncinate fasciculus FA
4	Mesial-inferior temporal	Entorhinal th. Parahippocampal th. Fusiform th. Temporal pole th.	Inferior longitudinal fasciculus FA
5	Superior-lateral temporal	Superior temporal th. Middle temporal th. Inferior temporal th. Transverse temporal th. Banks of the superior temporal sulcus th.	Average temporal FA
6	Parietal	Inferior parietal th. Superior parietal th. Supramarginal th. Precuneus th. Posterior cingulate th. Isthmus cingulate th.	Average parietal FA
7	Occipital	Lateral occipital th. Lingual th. Cuneus th. Pericalcarine th.	Average occipital FA
8	Motor	Precentral th. Paracentral th.	Corticospinal tract FA
9	Commissural	Posterior, middle, central, mid-anterior, anterior corpus callosum vol.	Forceps major FA Forceps minor FA Body of corpus callosum FA
10	Brainstem	Medulla vol., pons vol., midbrain vol	Brainstem FA
11	Cerebellum	Cerebellar cortex vol., superior cerebellar peduncle vol.	Inferior cerebellar peduncle FA, middle cerebellar peduncle FA, superior cerebellar peduncle FA, average cerebellar FA
12	Subcortical	Thalamus vol., caudate vol., putamen vol., pallidum vol., accumbens vol.	Anterior thalamic radiation FA, posterior thalamic radiation FA
13	Limbic	Amygdala vol., hippocampus vol.	Fornix FA Cingulum FA
14	Long association fibres	–	Inferior fronto-occipital fasciculus FA, superior longitudinal fasciculus FA
15	Sensory	Postcentral gyrus	Medial lemniscus FA

ROI region-of-interest, *FA* fractional anisotropy, *th.* thickness, *vol.* volume

analyses, the clinical and genetic profiles of the clusters were contrasted.

Results

Two-step cluster analysis identified two distinct clusters of anatomical disease-burden distribution, 35.5% of patients ($n = 76$) segregating to Cluster 1 and 64.5% ($n = 138$) to Cluster 2. The silhouette coefficient of 0.572 indicates

reasonable cohesion and separation according to Kaufman and Rousseeuw [32]. Variable ranking revealed that the ROIs that best predict cluster membership are superior lateral temporal, inferior frontal, superior frontal, parietal, limbic, mesial inferior temporal, peri-Sylvian, subcortical, long association fibres, commissural, occipital, 'sensory', 'motor', cerebellum, and brainstem in descending order of importance (Fig. 1).

To illustrate the discrimination potential of the anatomical regions between the clusters, a scatter plot was generated based on the integrity of the three most relevant anatomical regions (Fig. 2).

Based on allocated cluster membership, the demographic, clinical and genetic profiles of the two clusters were evaluated; *Cluster 1*: $n = 76$ age: 61.9 ± 11.9, male: 54 (71.1%), right handed: 73 (96.1%), education 13.5 ± 3.2, spinal onset: 67 (88.2%), ALSFRS-r: 37.9 ± 5.4, impaired on ECAS: 20 [26.3% of subjects in the cluster, 29.8% of subjects with ECAS available in the cluster ($n = 67$)], ALS-FTD: 13 (17.1%), *C9orf72* hexanucleotide carriers: 16 (21.1% of cluster).

Cluster 2: n = 138, age: 60.5 ± 11.9, male: 86 (62.3%), right handed: 129 (93.5%), education 14.1 ± 3.3, spinal onset: 119 (86.2%), ALSFRS-r: 38.8 ± 6.2, impaired on ECAS: 21 (15.2% of subjects in the cluster, 17.9% of subjects with ECAS available in the cluster ($n = 117$)), ALS-FTD: 15 (10.9%), *C9orf72* hexanucleotide carriers: 6 (4.3% of cluster). The two clusters were matched for age ($p = 0.39$), sex ($\chi^2_{corr.} = 1.29$, $p = 0.256$), handedness ($\chi^2_{corr.} = 0.22$, $p = 0.64$), education ($p = 0.25$), site of symptom onset ($\chi^2_{corr.} = 0.35$, $p = 0.85$), ALSFRS-r ($p = 0.28$), presence of comorbid FTD ($\chi 2_{corr.} = 1.17$, $p = 0.28$), and the proportion of patients with impairment on ECAS

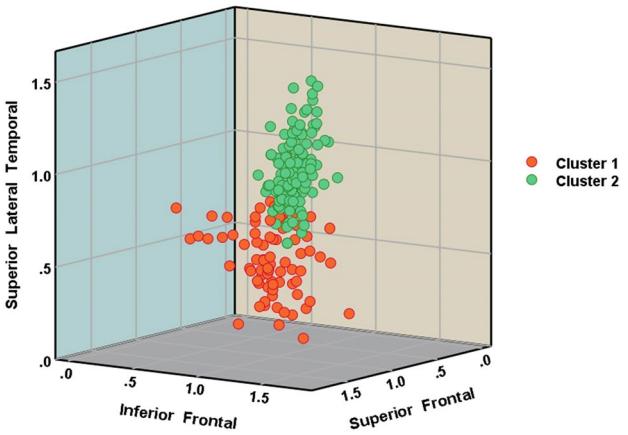

Fig. 2 3D scatter plot of patients in Cluster 1 and Cluster 2 based on the integrity of the superior lateral temporal, inferior frontal and parietal ROI

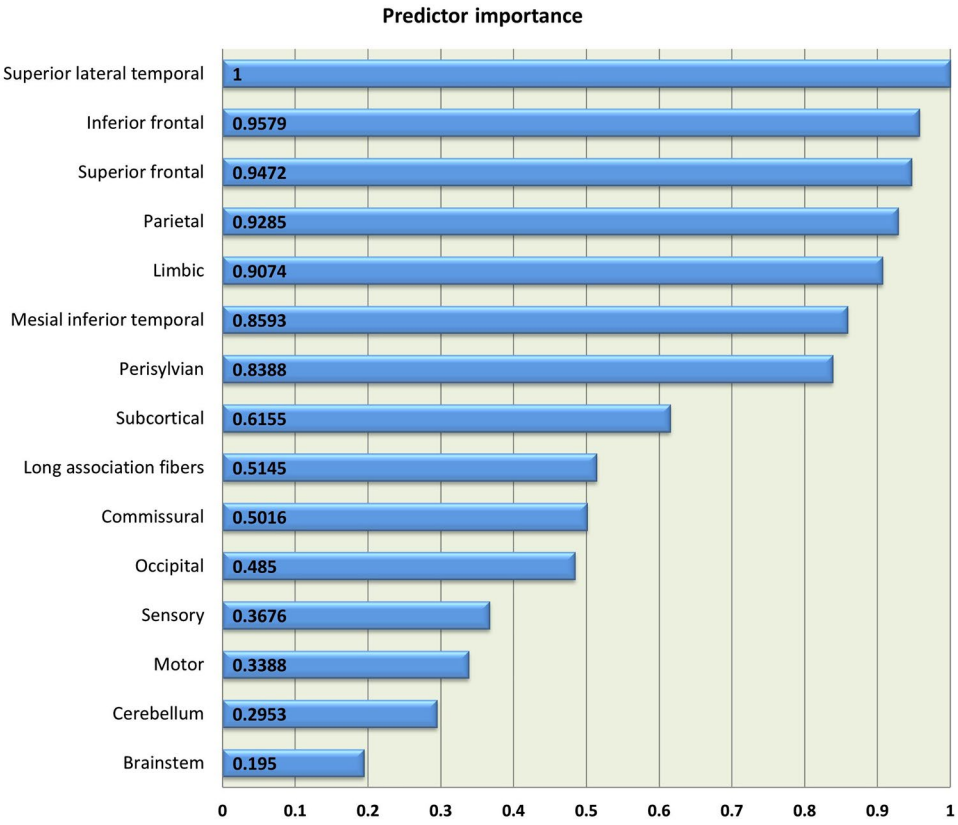

Fig. 1 The relative predictor importance profile of each anatomical region

($\chi 2_{corr.} = 3.99$, $p = 0.136$). The two clusters differed in genetic profiles ($\chi 2_{corr.} = 23.17$, $p < 0.0001$). In Cluster 1, there were 16 hexanucleotide repeat carriers which is 23.5% of patients with genetic information available in the cluster ($n = 68$). In Cluster 2, there were only six hexanucleotide repeat carriers which is 6.5% of patients with genetic information available in the cluster ($n = 93$). Of the 22 hexanucleotide carriers included in the study, 72.7% ($n = 16$) clustered to Cluster 1, and only 27.3% ($n = 6$) to Cluster 2.

Discussion

Our data confirm the radiological clustering of ALS into two relatively distinct subtypes. Contrary to previous staging or classification studies, we have not incorporated any complementary clinical, demographic or genetic information and uncovered two distinct subtypes based on the anatomical distribution of degenerative change alone in a large cohort of pooled ALS patients. The motivation behind our approach was to solely interpret objective, quantitative, spatially coded radiological data without applying any a priori stratification strategy. Whilst most studies first categorise patients based on clinical, genetic or phenotypic criteria to then describe phenotype- or genotype-associated imaging signatures, our intention was the opposite; evaluate the natural segregation of patients based on pathological patterns and then assess clinical features associated with the clusters.

Using cerebral grey and white matte measures in 15 cerebral regions covering the entire brain, we have detected 2 distinct subgroups: a larger cluster (64.5%) of patients with moderate extra-motor disease burden and a smaller cluster (35.5%) with considerable frontotemporal pathology. One of the objectives of the study was to evaluate which brain regions best distinguish the subgroups; therefore, the evaluation of predictor importance is of particular interest. The marked involvement of superior lateral temporal and frontal regions in a subset of patients is consistent with previous reports, but the high predictor importance of parietal changes merits further discussion. ALS is not traditionally associated with preferential parietal atrophy [33]. Parietal changes have been sporadically described mostly in association with advanced disease, but our study suggests that parietal indices may help to segregate patients into subgroups. Predictor importance ranking also revealed that the involvement of brain regions traditionally associated with ALS, such as the motor cortex, corticospinal tracts, commissural structures and brainstem do not readily distinguish disease clusters as the pathology of these regions represent core, unifying features of disease [34, 35]. The low predictor importance of the cerebellum is also of interest. Cerebellar changes in ALS have only been recently characterised in detail [36] and the gravity of cerebellar changes are thought to be associated with specific genotypes and phenotypes [7, 37]. While an ALS-ataxia continuum was proposed by some, our data did not indicate the existence of a cluster of patients with marked cerebellar involvement without frontotemporal change.

The heterogeneity of limbic involvement is consistent with the vast body of neuropsychology and neuroimaging literature [38–40]. The importance of mesial inferior temporal structures in segregating ALS subtypes is consistent with the literature of medial temporal pathology in ALS and their contribution to cognitive deficits [18, 41]. Peri-Sylvian features ranked relatively high in our study, despite the left–right averaging of integrity variables. Peri-Sylvian regions are seldom assessed specifically in ALS, as the focus of imaging studies in ALS-FTD is often orbitofrontal, dorsolateral prefrontal and various temporal regions. Preferential insular and Broca's area degeneration have been previously described in association with *C9orf72* [42] but also often detected in whole-brain cortical thickness or morphometric analyses. Language deficits in ALS are also relatively well described [43, 44], but rarely linked to focal degenerative change [45]. Subcortical integrity metrics ranked to the middle of predictor hierarchy which is somewhat unexpected given the role of subcortical structures driving neuropsychological manifestations and the notion that hexanucleotide carriers may exhibit particularly marked subcortical degeneration [46–49]. Sensory areas ranked low in their importance of separating the clusters, despite recent reports of subtle or subclinical sensory deficits in ALS [50, 51]. Our predictor analysis outcomes highlight the importance of systematically assessing each brain region in ALS instead of only pursuing the analysis of brain regions which are known to be affected based on post mortem data. Certain anatomical areas such as the parietal lobes and occipital lobe may not be characteristic regions of degeneration, yet, as illustrated, may have a role in segregating specific ALS subtypes. This observation is consistent with the emerging machine-learning literature of ALS [52, 53] which suggests that feature importance analyses, especially in multi-class classification schemes, may identify brain regions which are not classically associated with ALS [54, 55].

Our data indicate a relative discordance between clinical and radiological profiles. While subjects in Cluster 1 exhibited marked frontotemporal change radiologically and the proportion of patients with cognitive impairment was higher, the statistical comparison of clinical variables in the two clusters did not reach significance. Furthermore, the two clusters were also matched in motor disability as indicated by their ALSFRS-r profiles. The dissociation between disease burden and clinical performance is increasingly recognised [56] and a multitude of factors, such as compensatory processes, "motor reserve" and "cognitive reserve" may contribute [57–59]. The relative

genetic segregation of subjects based on their imaging profiles is of particular interest; 72.7% of hexanucleotide carriers segregated to Cluster 1, and only 27.3% to Cluster 2. It is conceivable, that in much larger datasets, imaging may have a role in uncovering anatomically unique subgroups which may carry a higher percentage of specific genetic variants or groups with distinct clinical features.

Our study is not without limitations. A silhouette coefficient of 0.572 can only be interpreted as a "reasonable" structure [32]. Our cluster analysis relied on cross-sectional data, and similarly to other studies [53, 60], the clinical implications of cluster membership need to be characterised further with regards to potential prognostic and survival ramifications. The assessment whether radiological cluster membership is consistent longitudinally throughout the course of the disease would be of interest [61]. Furthermore, only very basic clinical variables were appraised in the resulting anatomical clusters such as composite disability scores and cognitive screening outcomes. The fine-grained assessment of specific clinical domains such as pyramidal, extrapyramidal, cerebellar, language, social cognition, and apathy scores may reveal significant inter-cluster differences [4, 5, 62–64]. To explore patient segregation into core pathological patterns, relatively large anatomical regions were defined and only structural integrity metrics evaluated. The incorporation of spinal cord metrics [65, 66] and functional network integrity indices [17, 67] may have helped to identify additional clusters. Only symptomatic patients with an established diagnosis of ALS were included in this study. Given the considerable evidence of brain [44, 68] and spinal cord [69] alterations long before symptom onset, the anatomical clustering of asymptomatic mutation carriers would be of particular interest. Finally, the inclusion of non-ALS MNDs, such as SBMA, SMA, PLS, PPS or PMA in cluster analyses may be of potential interest to evaluate if these subtypes segregate from ALS based on their radiological profiles [70–76]. Notwithstanding these limitations, our study demonstrates that pooled radiology data may be utilised to uncover disease subtypes which may be associated with unique genetic profiles.

Conclusions

Cluster analysis of imaging data reveals distinct subtypes in ALS without accompanying clinical information. The interrogation of biomarkers by data-driven approaches helps to explore the heterogeneity of neurodegenerative conditions without a priori patient stratification. With the increased availability of large harmonised datasets, similar analyses may expose unique disease subtypes with distinctive clinical, prognostic or genetic traits.

Acknowledgements We are most thankful for the participation of each patient, and we also thank all the patients who expressed interest in this research study but were unable to participate for medical or logistical reasons. We also express our gratitude to the caregivers of ALS patients for facilitating attendance at our research centre. Without their generosity, this study would have not been possible.

Author contribution Drafting the manuscript: PB and KMC. Neuroimaging analyses: PB, AM, JL, and KMC. Conceptualisation of the study: PB and KMC. Revision of the manuscript for intellectual content: PB, AM, JL, OH, and KMC.

Funding Open Access funding provided by the IReL Consortium. Peter Bede and the Computational Neuroimaging Group are supported by the Health Research Board (HRB EIA-2017-019 and HRB JPND-CoFund2-2019-1), the Irish Institute of Clinical Neuroscience (IICN), the Spastic Paraplegia Foundation (SPF), the EU Joint Programme—Neurodegenerative Disease Research (JPND), the Andrew Lydon scholarship, and the Iris O'Brien Foundation.

Declarations

Conflicts of interest The authors have no competing interests to declare.

Ethics approval This study was approved by the Ethics (Medical Research) Committee—Beaumont Hospital, Dublin, Ireland.

References

1. Sarro L, Agosta F, Canu E, Riva N, Prelle A, Copetti M, Riccitelli G, Comi G, Filippi M (2011) Cognitive functions and white matter tract damage in amyotrophic lateral sclerosis: a diffusion tensor tractography study. AJNR Am J Neuroradiol 32(10):1866–1872. https://doi.org/10.3174/ajnr.A2658
2. Trojsi F, Di Nardo F, Caiazzo G, Siciliano M, D'Alvano G, Passaniti C, Russo A, Bonavita S, Cirillo M, Esposito F, Tedeschi G (2021) Between-sex variability of resting state functional brain networks in amyotrophic lateral sclerosis (ALS). J Neural Transm (Vienna) 128(12):1881–1897. https://doi.org/10.1007/s00702-021-02413-0
3. Spinelli EG, Agosta F, Canu E, Ferraro PM, Riva N, Copetti M, Chiò A, Messina S, Iannaccone S, Calvo A, Silani V, Falini A, Comi G, Filippi M (2014) Cognitive changes and white matter

tract damage in the motor neuron disease spectrum. J Neurol 261:S48. https://doi.org/10.1007/s00415-014-7337-4
4. Burke T, Pinto-Grau M, Lonergan K, Elamin M, Bede P, Costello E, Hardiman O, Pender N (2016) Measurement of social cognition in amyotrophic lateral sclerosis: a population based study. PLoS ONE 11(8):e0160850. https://doi.org/10.1371/journal.pone.0160850
5. Abidi M, de Marco G, Grami F, Termoz N, Couillandre A, Querin G, Bede P, Pradat PF (2021) Neural correlates of motor imagery of gait in amyotrophic lateral sclerosis. J Magn Reson Imaging 53(1):223–233. https://doi.org/10.1002/jmri.27335
6. Li Hi Shing S, Bede P (2021) The neuroradiology of upper motor neuron degeneration: PLS, HSP, ALS. Amyotroph Lateral Scler Front Degener. https://doi.org/10.1080/21678421.2021.1951293
7. Bede P, Chipika RH, Christidi F, Hengeveld JC, Karavasilis E, Argyropoulos GD, Lope J, Li Hi Shing S, Velonakis G, Dupuis L, Doherty MA, Vajda A, McLaughlin RL, Hardiman O (2021) Genotype-associated cerebellar profiles in ALS: focal cerebellar pathology and cerebro-cerebellar connectivity alterations. J Neurol Neurosurg Psychiatry 92(11):1197–1205. https://doi.org/10.1136/jnnp-2021-326854
8. Lule D, Diekmann V, Muller HP, Kassubek J, Ludolph AC, Birbaumer N (2010) Neuroimaging of multimodal sensory stimulation in amyotrophic lateral sclerosis. J Neurol Neurosurg Psychiatry 81(8):899–906. https://doi.org/10.1136/jnnp.2009.192260
9. Mitsumoto H, Brooks BR, Silani V (2014) Clinical trials in amyotrophic lateral sclerosis: why so many negative trials and how can trials be improved? Lancet Neurol 13(11):1127–1138. https://doi.org/10.1016/s1474-4422(14)70129-2
10. Fang T, Al Khleifat A, Stahl DR, Lazo La Torre C, Murphy C, Young C, Shaw PJ, Leigh PN, Al-Chalabi A (2017) Comparison of the King's and MiToS staging systems for ALS. Amyotroph Lateral Scler Front Degener 18(3–4):227–232. https://doi.org/10.1080/21678421.2016.1265565
11. Tramacere I, Dalla Bella E, Chio A, Mora G, Filippini G, Lauria G (2015) The MITOS system predicts long-term survival in amyotrophic lateral sclerosis. J Neurol Neurosurg Psychiatry 86(11):1180–1185. https://doi.org/10.1136/jnnp-2014-310176
12. Brooks BR, Miller RG, Swash M, Munsat TL, Gr WFNR (2000) El Escorial revisited: revised criteria for the diagnosis of amyotrophic lateral sclerosis. Amyotroph Lateral Sc 1(5):293–299
13. Strong MJ, Grace GM, Freedman M, Lomen-Hoerth C, Woolley S, Goldstein LH, Murphy J, Shoesmith C, Rosenfeld J, Leigh PN, Bruijn L, Ince P, Figlewicz D (2009) Consensus criteria for the diagnosis of frontotemporal cognitive and behavioural syndromes in amyotrophic lateral sclerosis. Amyotroph Lateral Scler 10(3):131–146. https://doi.org/10.1080/17482960802654364
14. Balendra R, Jones A, Jivraj N, Steen IN, Young CA, Shaw PJ, Turner MR, Leigh PN, Al-Chalabi A (2015) Use of clinical staging in amyotrophic lateral sclerosis for phase 3 clinical trials. J Neurol Neurosurg Psychiatry 86(1):45–49. https://doi.org/10.1136/jnnp-2013-306865
15. Devos D, Moreau C, Kyheng M, Garcon G, Rolland AS, Blasco H, Gele P, Timothee Lenglet T, Veyrat-Durebex C, Corcia P, Dutheil M, Bede P, Jeromin A, Oeckl P, Otto M, Meninger V, Danel-Brunaud V, Devedjian JC, Duce JA, Pradat PF (2019) A ferroptosis-based panel of prognostic biomarkers for Amyotrophic Lateral Sclerosis. Sci Rep 9(1):2918. https://doi.org/10.1038/s41598-019-39739-5
16. Blasco H, Patin F, Descat A, Garcon G, Corcia P, Gele P, Lenglet T, Bede P, Meininger V, Devos D, Gossens JF, Pradat PF (2018) A pharmaco-metabolomics approach in a clinical trial of ALS: identification of predictive markers of progression. PLoS ONE 13(6):e0198116. https://doi.org/10.1371/journal.pone.0198116
17. Dukic S, McMackin R, Buxo T, Fasano A, Chipika R, Pinto-Grau M, Costello E, Schuster C, Hammond M, Heverin M, Coffey A, Broderick M, Iyer PM, Mohr K, Gavin B, Pender N, Bede P, Muthuraman M, Lalor EC, Hardiman O, Nasseroleslami B (2019) Patterned functional network disruption in amyotrophic lateral sclerosis. Hum Brain Mapp 40(16):4827–4842. https://doi.org/10.1002/hbm.24740
18. Christidi F, Karavasilis E, Rentzos M, Velonakis G, Zouvelou V, Xirou S, Argyropoulos G, Papatriantafyllou I, Pantolewn V, Ferentinos P, Kelekis N, Seimenis I, Evdokimidis I, Bede P (2019) Hippocampal pathology in amyotrophic lateral sclerosis: selective vulnerability of subfields and their associated projections. Neurobiol Aging 84:178–188. https://doi.org/10.1016/j.neurobiolaging.2019.07.019
19. Finegan E, Li Hi Shing S, Chipika RH, Doherty MA, Hengeveld JC, Vajda A, Donaghy C, Pender N, McLaughlin RL, Hardiman O, Bede P (2019) Widespread subcortical grey matter degeneration in primary lateral sclerosis: a multimodal imaging study with genetic profiling. NeuroImage Clinical 24:102089. https://doi.org/10.1016/j.nicl.2019.102089
20. Chipika RH, Siah WF, Shing SLH, Finegan E, McKenna MC, Christidi F, Chang KM, Karavasilis E, Vajda A, Hengeveld JC, Doherty MA, Donaghy C, Hutchinson S, McLaughlin RL, Hardiman O, Bede P (2020) MRI data confirm the selective involvement of thalamic and amygdalar nuclei in amyotrophic lateral sclerosis and primary lateral sclerosis. Data Brief. https://doi.org/10.1016/j.dib.2020.106246
21. Fischl B (2012) FreeSurfer. Neuroimage 62(2):774–781. https://doi.org/10.1016/j.neuroimage.2012.01.021
22. Schuster C, Hardiman O, Bede P (2016) Development of an automated mri-based diagnostic protocol for amyotrophic lateral sclerosis using disease-specific pathognomonic features: a quantitative disease-state classification study. PLoS ONE 11(12):e0167331. https://doi.org/10.1371/journal.pone.0167331
23. Iglesias JE, Van Leemput K, Bhatt P, Casillas C, Dutt S, Schuff N, Truran-Sacrey D, Boxer A, Fischl B (2015) Bayesian segmentation of brainstem structures in MRI. Neuroimage 113:184–195. https://doi.org/10.1016/j.neuroimage.2015.02.065
24. Mori S, Oishi K, Jiang H, Jiang L, Li X, Akhter K, Hua K, Faria AV, Mahmood A, Woods R, Toga AW, Pike GB, Neto PR, Evans A, Zhang J, Huang H, Miller MI, van Zijl P, Mazziotta J (2008) Stereotaxic white matter atlas based on diffusion tensor imaging in an ICBM template. Neuroimage 40(2):570–582. https://doi.org/10.1016/j.neuroimage.2007.12.035
25. Mori S, Wakana S, Van Zijl P, Nagae-Poetscher L (2005) MRI atlas of human white matter. Elsevier, The Netherlands
26. Wakana S, Caprihan A, Panzenboeck MM, Fallon JH, Perry M, Gollub RL, Hua K, Zhang J, Jiang H, Dubey P, Blitz A, van Zijl P, Mori S (2007) Reproducibility of quantitative tractography methods applied to cerebral white matter. Neuroimage 36(3):630–644. https://doi.org/10.1016/j.neuroimage.2007.02.049
27. Hua K, Zhang J, Wakana S, Jiang H, Li X, Reich DS, Calabresi PA, Pekar JJ, van Zijl PC, Mori S (2008) Tract probability maps in stereotaxic spaces: analyses of white matter anatomy and tract-specific quantification. Neuroimage 39(1):336–347. https://doi.org/10.1016/j.neuroimage.2007.07.053
28. Brown CA, Johnson NF, Anderson-Mooney AJ, Jicha GA, Shaw LM, Trojanowski JQ, Van Eldik LJ, Schmitt FA, Smith CD, Gold BT (2017) Development, validation and application of a new fornix template for studies of aging and preclinical Alzheimer's disease. NeuroImage Clin 13:106–115. https://doi.org/10.1016/j.nicl.2016.11.024
29. Collins DL, Holmes CJ, Peters TM, Evans AC (1995) Automatic 3-D model-based neuroanatomical segmentation. Hum Brain Mapp 3(3):190–208. https://doi.org/10.1002/hbm.460030304

30. Mazziotta J, Toga A, Evans A, Fox P, Lancaster J, Zilles K, Woods R, Paus T, Simpson G, Pike B, Holmes C, Collins L, Thompson P, MacDonald D, Iacoboni M, Schormann T, Amunts K, Palomero-Gallagher N, Geyer S, Parsons L, Narr K, Kabani N, Le Goualher G, Boomsma D, Cannon T, Kawashima R, Mazoyer B (2001) A probabilistic atlas and reference system for the human brain: International Consortium for Brain Mapping (ICBM). Philos Trans R Soc Lond B Biol Sci 356(1412):1293–1322. https://doi.org/10.1098/rstb.2001.0915
31. Desikan RS, Segonne F, Fischl B, Quinn BT, Dickerson BC, Blacker D, Buckner RL, Dale AM, Maguire RP, Hyman BT, Albert MS, Killiany RJ (2006) An automated labeling system for subdividing the human cerebral cortex on MRI scans into gyral based regions of interest. Neuroimage 31(3):968–980. https://doi.org/10.1016/j.neuroimage.2006.01.021
32. Kaufman L, Rousseeuw P (1990) Finding groups in data: an introduction to cluster analysis. https://doi.org/10.2307/2532178
33. Bede P, Iyer PM, Schuster C, Elamin M, McLaughlin RL, Kenna K, Hardiman O (2016) The selective anatomical vulnerability of ALS: "disease-defining" and "disease-defying" brain regions. Amyotroph Lateral Scler Front Degener 17(7–8):561–570. https://doi.org/10.3109/21678421.2016.1173702
34. Bede P, Chipika RH, Finegan E, Li Hi Shing S, Doherty MA, Hengeveld JC, Vajda A, Hutchinson S, Donaghy C, McLaughlin RL, Hardiman O (2019) Brainstem pathology in amyotrophic lateral sclerosis and primary lateral sclerosis: a longitudinal neuroimaging study. NeuroImage Clin 24:102054. https://doi.org/10.1016/j.nicl.2019.102054
35. Muller HP, Turner MR, Grosskreutz J, Abrahams S, Bede P, Govind V, Prudlo J, Ludolph AC, Filippi M, Kassubek J (2016) A large-scale multicentre cerebral diffusion tensor imaging study in amyotrophic lateral sclerosis. J Neurol Neurosurg Psychiatry 87(6):570–579. https://doi.org/10.1136/jnnp-2015-311952
36. Tu S, Menke RAL, Talbot K, Kiernan MC, Turner MR (2019) Cerebellar tract alterations in PLS and ALS. Amyotroph Lateral Scler Front Degener 20(3–4):281–284. https://doi.org/10.1080/21678421.2018.1562554
37. Tan RH, Kril JJ, McGinley C, Hassani M, Masuda-Suzukake M, Hasegawa M, Mito R, Kiernan MC, Halliday GM (2016) Cerebellar neuronal loss in amyotrophic lateral sclerosis cases with ATXN2 intermediate repeat expansions. Ann Neurol 79(2):295–305. https://doi.org/10.1002/ana.24565
38. Burke T, Lonergan K, Pinto-Grau M, Elamin M, Bede P, Madden C, Hardiman O, Pender N (2017) Visual encoding, consolidation, and retrieval in amyotrophic lateral sclerosis: executive function as a mediator, and predictor of performance. Amyotroph Lateral Scler Front Degener 18(3–4):193–201. https://doi.org/10.1080/21678421.2016.1272615
39. Trojsi F, Di Nardo F, Santangelo G, Siciliano M, Femiano C, Passaniti C, Caiazzo G, Fratello M, Cirillo M, Monsurrò MR, Esposito F, Tedeschi G (2017) Resting state fMRI correlates of Theory of Mind impairment in amyotrophic lateral sclerosis. Cortex 97:1–16. https://doi.org/10.1016/j.cortex.2017.09.016
40. Lule D, Diekmann V, Anders S, Kassubek J, Kubler A, Ludolph AC, Birbaumer N (2007) Brain responses to emotional stimuli in patients with amyotrophic lateral sclerosis (ALS). J Neurol 254(4):519–527
41. Chipika RH, Christidi F, Finegan E, Li Hi Shing S, McKenna MC, Chang KM, Karavasilis E, Doherty MA, Hengeveld JC, Vajda A, Pender N, Hutchinson S, Donaghy C, McLaughlin RL, Hardiman O, Bede P (2020) Amygdala pathology in amyotrophic lateral sclerosis and primary lateral sclerosis. J Neurol Sci 417:117039. https://doi.org/10.1016/j.jns.2020.117039
42. Bede P, Bokde AL, Byrne S, Elamin M, McLaughlin RL, Kenna K, Fagan AJ, Pender N, Bradley DG, Hardiman O (2013) Multiparametric MRI study of ALS stratified for the C9orf72 genotype. Neurology 81(4):361–369. https://doi.org/10.1212/WNL.0b013e31829c5eee
43. Taylor LJ, Brown RG, Tsermentseli S, Al-Chalabi A, Shaw CE, Ellis CM, Leigh PN, Goldstein LH (2013) Is language impairment more common than executive dysfunction in amyotrophic lateral sclerosis? J Neurol Neurosurg Psychiatry 84(5):494–498
44. Lulé DE, Müller HP, Finsel J, Weydt P, Knehr A, Winroth I, Andersen P, Weishaupt J, Uttner I, Kassubek J, Ludolph AC (2020) Deficits in verbal fluency in presymptomatic C9orf72 mutation gene carriers-a developmental disorder. J Neurol Neurosurg Psychiatry 91(11):1195–1200. https://doi.org/10.1136/jnnp-2020-323671
45. Omer T, Finegan E, Hutchinson S, Doherty M, Vajda A, McLaughlin RL, Pender N, Hardiman O, Bede P (2017) Neuroimaging patterns along the ALS-FTD spectrum: a multiparametric imaging study. Amyotroph Lateral Scleros Front Degener 18(7–8):611–623. https://doi.org/10.1080/21678421.2017.1332077
46. Trojsi F, Di Nardo F, Caiazzo G, Siciliano M, D'Alvano G, Ferrantino T, Passaniti C, Ricciardi D, Esposito S, Lavorgna L, Russo A, Bonavita S, Cirillo M, Santangelo G, Esposito F, Tedeschi G (2020) Hippocampal connectivity in Amyotrophic Lateral Sclerosis (ALS): more than Papez circuit impairment. Brain Imaging Behav. https://doi.org/10.1007/s11682-020-00408-1
47. Bede P, Omer T, Finegan E, Chipika RH, Iyer PM, Doherty MA, Vajda A, Pender N, McLaughlin RL, Hutchinson S, Hardiman O (2018) Connectivity-based characterisation of subcortical grey matter pathology in frontotemporal dementia and ALS: a multimodal neuroimaging study. Brain Imaging Behav 12(6):1696–1707. https://doi.org/10.1007/s11682-018-9837-9
48. Christidi F, Karavasilis E, Velonakis G, Ferentinos P, Rentzos M, Kelekis N, Evdokimidis I, Bede P (2018) The clinical and radiological spectrum of hippocampal pathology in amyotrophic lateral sclerosis. Front Neurol 9:523. https://doi.org/10.3389/fneur.2018.00523
49. Christidi F, Karavasilis E, Rentzos M, Kelekis N, Evdokimidis I, Bede P (2018) Clinical and radiological markers of extra-motor deficits in amyotrophic lateral sclerosis. Front Neurol 9:1005. https://doi.org/10.3389/fneur.2018.01005
50. Chipika RH, Mulkerrin G, Murad A, Lope J, Hardiman O, Bede P (2022) Alterations in somatosensory, visual and auditory pathways in amyotrophic lateral sclerosis: an under-recognised facet of ALS. J Integr Neurosci 1–18 (In Press)
51. Cohen-Adad J, El Mendili MM, Morizot-Koutlidis R, Lehericy S, Meininger V, Blancho S, Rossignol S, Benali H, Pradat PF (2013) Involvement of spinal sensory pathway in ALS and specificity of cord atrophy to lower motor neuron degeneration. Amyotroph Lateral Scler Front Degener 14(1):30–38. https://doi.org/10.3109/17482968.2012.701308
52. Grollemund V, Pradat PF, Querin G, Delbot F, Le Chat G, Pradat-Peyre JF, Bede P (2019) Machine learning in amyotrophic lateral sclerosis: achievements, pitfalls, and future directions. Front Neurosci 13:135. https://doi.org/10.3389/fnins.2019.00135
53. Grollemund V, Le Chat G, Secchi-Buhour MS, Delbot F, Pradat-Peyre JF, Bede P, Pradat PF (2021) Manifold learning for amyotrophic lateral sclerosis functional loss assessment: development and validation of a prognosis model. J Neurol 268(3):825–850. https://doi.org/10.1007/s00415-020-10181-2
54. Bede P, Murad A, Hardiman O (2021) Pathological neural networks and artificial neural networks in ALS: diagnostic classification based on pathognomonic neuroimaging features. J Neurol. https://doi.org/10.1007/s00415-021-10801-5
55. Bede P, Murad A, Lope J, Li Hi Shing S, Finegan E, Chipika RH, Hardiman O, Chang KM (2021) Phenotypic categorisation of individual subjects with motor neuron disease based on radiological

disease burden patterns: a machine-learning approach. J Neurol Sci 432:120079. https://doi.org/10.1016/j.jns.2021.120079
56. Verstraete E, Turner MR, Grosskreutz J, Filippi M, Benatar M (2015) Mind the gap: the mismatch between clinical and imaging metrics in ALS. Amyotroph Lateral Scler Front Degener 16(7–8):524–529. https://doi.org/10.3109/21678421.2015.1051989
57. Abidi M, de Marco G, Couillandre A, Feron M, Mseddi E, Termoz N, Querin G, Pradat PF, Bede P (2020) Adaptive functional reorganization in amyotrophic lateral sclerosis: coexisting degenerative and compensatory changes. Eur J Neurol 27(1):121–128. https://doi.org/10.1111/ene.14042
58. Bede P, Bogdahn U, Lope J, Chang KM, Xirou S, Christidi F (2021) Degenerative and regenerative processes in amyotrophic lateral sclerosis: motor reserve, adaptation and putative compensatory changes. Neural Regen Res 16(6):1208–1209. https://doi.org/10.4103/1673-5374.300440
59. Costello E, Rooney J, Pinto-Grau M, Burke T, Elamin M, Bede P, McMackin R, Dukic S, Vajda A, Heverin M, Hardiman O, Pender N (2021) Cognitive reserve in amyotrophic lateral sclerosis (ALS): a population-based longitudinal study. J Neurol Neurosurg Psychiatry. https://doi.org/10.1136/jnnp-2020-324992
60. Schuster C, Hardiman O, Bede P (2017) Survival prediction in Amyotrophic lateral sclerosis based on MRI measures and clinical characteristics. BMC Neurol 17(1):73. https://doi.org/10.1186/s12883-017-0854-x
61. Meier JM, van der Burgh HK, Nitert AD, Bede P, de Lange SC, Hardiman O, van den Berg LH, van den Heuvel MP (2020) Connectome-based propagation model in amyotrophic lateral sclerosis. Ann Neurol 87(5):725–738. https://doi.org/10.1002/ana.25706
62. Burke T, Elamin M, Bede P, Pinto-Grau M, Lonergan K, Hardiman O, Pender N (2016) Discordant performance on the "Reading the Mind in the Eyes" Test, based on disease onset in amyotrophic lateral sclerosis. Amyotroph Lateral Scler Front Degener 17(7–8):467–472. https://doi.org/10.1080/21678421.2016.1177088
63. Lule D, Pauli S, Altintas E, Singer U, Merk T, Uttner I, Birbaumer N, Ludolph AC (2012) Emotional adjustment in amyotrophic lateral sclerosis (ALS). J Neurol 259(2):334–341. https://doi.org/10.1007/s00415-011-6191-x
64. Feron M, Couillandre A, Mseddi E, Termoz N, Abidi M, Bardinet E, Delgadillo D, Lenglet T, Querin G, Welter ML, Le Forestier N, Salachas F, Bruneteau G, Del Mar AM, Debs R, Lacomblez L, Meininger V, Pelegrini-Issac M, Bede P, Pradat PF, de Marco G (2018) Extrapyramidal deficits in ALS: a combined biomechanical and neuroimaging study. J Neurol 265(9):2125–2136. https://doi.org/10.1007/s00415-018-8964-y
65. El Mendili MM, Querin G, Bede P, Pradat PF (2019) Spinal cord imaging in amyotrophic lateral sclerosis: historical concepts-novel techniques. Front Neurol 10:350. https://doi.org/10.3389/fneur.2019.00350
66. Querin G, El Mendili MM, Bede P, Delphine S, Lenglet T, Marchand-Pauvert V, Pradat PF (2018) Multimodal spinal cord MRI offers accurate diagnostic classification in ALS. J Neurol Neurosurg Psychiatry 89(11):1220–1221. https://doi.org/10.1136/jnnp-2017-317214
67. Proudfoot M, Bede P, Turner MR (2018) Imaging cerebral activity in amyotrophic lateral sclerosis. Front Neurol 9:1148. https://doi.org/10.3389/fneur.2018.01148
68. Chipika RH, Siah WF, McKenna MC, Li Hi Shing S, Hardiman O, Bede P (2021) The presymptomatic phase of amyotrophic lateral sclerosis: are we merely scratching the surface? J Neurol 268(12):4607–4629. https://doi.org/10.1007/s00415-020-10289-5
69. Querin G, Bede P, El Mendili MM, Li M, Pelegrini-Issac M, Rinaldi D, Catala M, Saracino D, Salachas F, Camuzat A, Marchand-Pauvert V, Cohen-Adad J, Colliot O, Le Ber I, Pradat PF (2019) Presymptomatic spinal cord pathology in c9orf72 mutation carriers: a longitudinal neuroimaging study. Ann Neurol 86(2):158–167. https://doi.org/10.1002/ana.25520
70. Floeter MK, Mills R (2009) Progression in primary lateral sclerosis: a prospective analysis. Amyotroph Lateral Scler 10(5–6):339–346
71. Querin G, El Mendili MM, Lenglet T, Behin A, Stojkovic T, Salachas F, Devos D, Le Forestier N, Del Mar AM, Debs R, Lacomblez L, Meninger V, Bruneteau G, Cohen-Adad J, Lehericy S, Laforet P, Blancho S, Benali H, Catala M, Li M, Marchand-Pauvert V, Hogrel JY, Bede P, Pradat PF (2019) The spinal and cerebral profile of adult spinal-muscular atrophy: a multimodal imaging study. NeuroImage Clinical 21:101618. https://doi.org/10.1016/j.nicl.2018.101618
72. Finegan E, Chipika RH, Li Hi Shing S, Doherty MA, Hengeveld JC, Vajda A, Donaghy C, McLaughlin RL, Pender N, Hardiman O, Bede P (2019) The clinical and radiological profile of primary lateral sclerosis: a population-based study. J Neurol 266(11):2718–2733. https://doi.org/10.1007/s00415-019-09473-z
73. Li Hi Shing S, Chipika RH, Finegan E, Murray D, Hardiman O, Bede P (2019) Post-polio syndrome: more than just a lower motor neuron disease. Front Neurol 10:773. https://doi.org/10.3389/fneur.2019.00773
74. Tahedl M, Li Hi Shing S, Finegan E, Chipika RH, Lope J, Hardiman O, Bede P (2021) Propagation patterns in motor neuron diseases: individual and phenotype-associated disease-burden trajectories across the UMN-LMN spectrum of MNDs. Neurobiol Aging 109:78–87. https://doi.org/10.1016/j.neurobiolaging.2021.04.031
75. Pradat PF, Bernard E, Corcia P, Couratier P, Jublanc C, Querin G, Morelot Panzini C, Salachas F, Vial C, Wahbi K, Bede P, Desnuelle C (2020) The French national protocol for Kennedy's disease (SBMA): consensus diagnostic and management recommendations. Orphanet J Rare Dis 15(1):90. https://doi.org/10.1186/s13023-020-01366-z
76. Spinelli EG, Agosta F, Ferraro PM, Riva N, Lunetta C, Falzone YM, Comi G, Falini A, Filippi M (2016) Brain MR imaging in patients with lower motor neuron-predominant disease. Radiology 280(2):545–556. https://doi.org/10.1148/radiol.2016151846